

Accelerated Synthesis and Analysis of NiO, ZnO, and ZnO/NiO Materials for Prospective Applications

Akumarti Raju, Vangapandu Anusha, Budithi Ravi Kumar, Gattupalli Manikya Rao*

*Department of Physics, Andhra University, Visakhapatnam-530003, Andhra Pradesh.
Email: dr.gmanikyarao@andhrauniversity.edu.in*

This work demonstrates a straightforward, inexpensive, and rapid route for the synthesis of nickel oxide (NiO), Zinc Oxide (ZnO), and its composite (ZnO/NiO) nanoparticles through the green method using Azadirachta indica (Neem) leaves. The structure, morphology, and elemental constituents were characterized by X-ray diffraction, scanning electron microscopy, and energy-dispersive X-ray spectroscopy. The energy band gap of pure NiO, ZnO, and ZnO/NiO composite was evaluated using the Tauc plot from absorption spectra and resulted as 4.6, 5.1, and 5.2 eV, respectively. The prominent functional groups identified by Fourier-transform infrared (FTIR) spectroscopy. Therefore, comparatively individual NiO and ZnO, semiconducting composite-based nanocatalysts such as ZnO/NiO composites are promising for future industrial applications.

Keywords: Green Synthesis, Azadirachta indica leaves, Nickel Oxide (NiO), Zinc Oxide (ZnO), ZnO/NiO Nanocomposites.

1. Introduction

NiO-ZnO composites are fascinating materials with many applications, particularly in energy storage and environmental remediation [1]. NiO-ZnO composites are hybrid materials combining nickel oxide (NiO) and Zinc oxide (ZnO) nanostructures. NiO and ZnO are the most studied pseudocapacitive materials, exhibiting reversible redox reactions allowing high-energy storage [1-2]. Combining these two oxides into a nanocomposite can synergistically enhance the electrochemical performance by leveraging the unique properties of each material. These composites exhibit improved properties compared to their components, making them attractive for various applications such as Photocatalysis, Gas sensing, Electrochemical applications, Antibacterial properties, Optical properties, and

Magnetic properties. NiO-ZnO nanocomposites can display interesting magnetic behavior, depending on composition and synthesis method [3-4]. Synthesis methods for NiO-ZnO composites include the sol-gel process, Hydrothermal synthesis, Co-precipitation, Electrospinning, and Chemical vapor deposition. Research on NiO-ZnO composites focuses on optimizing synthesis methods, understanding structure-property relationships, and exploring new applications in environmental remediation, energy storage, and biomedical technologies [5-6]. The rapid growth of energy consumption and the instability of renewable energy sources have highlighted an urge to develop efficient, high-performance energy storage systems [7].

Herein, ZnO, NiO, and ZnO/NiO materials were synthesized using a simple green method. The varied instrumental techniques are focused on studying the characteristic features. For comparative purposes, pristine NiO and ZnO were also evaluated. Finally, the composites are expected to offer more prominent Potential applications.

2. Experimental

2.1 Materials

Azadirachtaindica (Neem) leaves, Zinc acetate dihydrate ($\text{Zn}(\text{CH}_3\text{CO}_2)_2 \cdot 2\text{H}_2\text{O}$), Nickel acetate dihydrate ($\text{C}_4\text{H}_{12}\text{NiO}_6$) and Sodium Hydroxide (NaOH). All the chemicals were used as received without any further purification.

2.2 Green synthesis of ZnO/NiO nanocomposite

The NiO/ZnO nanocomposite was synthesized by following a green method described by [8]. The green route is an eco-friendly and cost-effective approach to replacing highly toxic and hazardous chemicals. In brief, Azadirachtaindica (Neem) leaves were collected and washed with tap water and then distilled to remove dust particles. The cleaned leaves were dried in a hot air oven at 35°C for 2 hours. Next, 10 grams of the dried leaves were boiled in 100 mL of distilled water at 70°C for 30 minutes and filtered through Whatman filter paper. The resulting leaf extract was stored at 4°C in a refrigerator for later use in synthesizing ZnO, NiO, and ZnO/NiO composites.

For synthesizing the ZnO/NiO composite via a green method, 25 mL of A. indica leaf extract was mixed with 50 mL of distilled water in two separate beakers and stirred with a magnetic stirrer at 60°C for 30 minutes. Then, 0.2 M Zinc acetate dihydrate and 0.2 M Nickel acetate dihydrate were added to the solutions containing the leaf extract and stirred under the same conditions. The Zinc acetate dihydrate solution was gradually added to the Nickel acetate dihydrate solution with continuous stirring. The pH of the solution was adjusted to ~7 using 0.5M NaOH aqueous solution, and the mixture was stirred for an additional 6 hours. The precipitate was centrifuged at 3500 rpm for 10 minutes and washed with distilled water and ethanol to remove impurities. The residue was dried in an oven for 6 hours at 60°C and annealed in a programmable furnace at 500°C for 2 hours. Finally, the ZnO/NiO nanocomposite powder was obtained. A similar procedure was used to synthesize pure ZnO and NiO nanomaterials.

2.3 Characterization Techniques

The surface morphology of the synthesized samples was analyzed by a field emission scanning electron microscope (FE-SEM, Carl Zeiss, Ultra Plus). The sample was attached to the carbon tape for the FE-SEM analysis. X-ray diffraction (XRD) (Bruker D8 advance) identified the crystallinity of the synthesized samples. Fourier recognized the functional groups in the as-prepared samplestransform infrared spectroscopy analysis (FTIR-4200). The optical absorption of samples was recorded by a UV-visible spectrophotometer (Analytical Jena, Specord 210 Plus).

3. Results and discussion

3.1. Characteristics of NiO, ZnO,and ZnO/NiO

3.1.1 Powder X-Ray Diffraction Study

Powder X-ray diffraction is the most helpful technique for phaseidentification and structural parameters of the synthesizedmaterials[9]. The X-ray diffraction patterns of ZnO/NiO and the individual phases ofZnO and NiO are depicted in Figure 1. The XRD pattern of NiO inFigure 1 showed that the synthesized material revealedsharpened peaks, indicating the crystallinity of NiO. Thepeaks positioned appearing at 2θ values of 37.35°, 43.40°,63.11°, 75.51°, and 79.45° and each peak is designated as (111),(200), (220), (311), and (222), respectively.These identifiedpeaks were well indexed to the cubic of the NiOphase (JCPDS cared no. 01-073-1519).Thediffraction peaks of ZnO located at 2θof 31.76°, 34.47°,36.23°,47.60°,56.69°,62.78°, 68.12°, and 69.27 indexed torelative planes (100), (002),(101), (102), (110), (103), (112), and (201) are matched to hexagonal phase(JCPDS No. 01-086-3978). The XRD patterns ofZnO/NiO composite contain peaks at 32.2°, 34.74°, 36.6°, 37.12, 43.25°,47.74°,56.95°, 63.03°, 68.20°,69.55°, and 75.24° indexed to hexagonal phase of ZnO crystal planes (100), (002), (101),(111),(102), (110), (103), (112),(220), (112), (201), and (202). These matched thestandard (JCPDS No. 01-080-6504) and agreed with thehexagonal phase. The significant peaks (111), (200), and (220) of NiO appear in the composite pattern. It confirms the excellent bonding between metal oxides and the maintained hexagonal phase. The average crystallite sizes of NiO, ZnO, and ZnO/NiO materials obtained from the Scherrer equation are represented in Table 1. The average crystallite size of theseprepared materials was calculated by applying the Scherrerequation: $D = (K \lambda) / (\beta \cos \theta)$, where D is the average crystallitesize, $\lambda = 1.54056 \text{ \AA}$ is the wavelength of Cu $\text{K}\alpha$, β is the fullwidth at half-maximum (FWHM) intensity, θ is Bragg'sdiffraction angle, and K is a constant taken as to 0.94[10-12]. The calculated value in the table is that the averages of the crystallite size from the four peaks of each material are 11.56 nm, 27.32 nm, and 39.51nm NiO, ZnO, and ZnO/NiO, respectively. The average crystallite size of NiO is less than that ZnO and ZnO/NiO composites, possibly due to the mixed oxide formation in the composites

Sno.	Nanoparticles and its Composite	Average Crystalline Size[nm]
1.	NiO	11.56 nm
2.	ZnO	27.32 nm
3.	ZnO/NiO	39.51 nm

Table 1. Average Crystalline Size of NiO, ZnO and ZnO/NiO

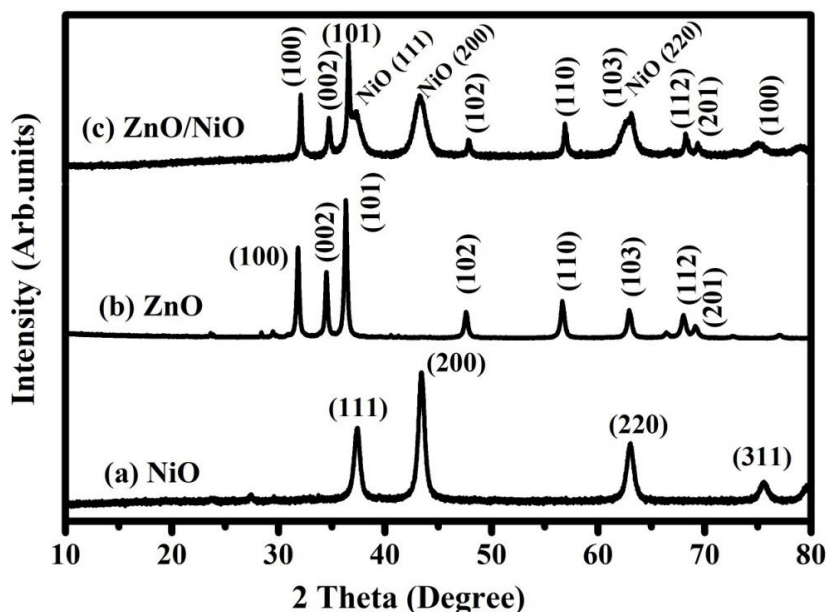


Fig.1. X-ray diffractograms of (a) NiO, (b) ZnO, and (c) ZnO/NiO

3.1.2 Morphology and Elemental Analysis

FESEM images of NiO, ZnO, and NiO/ZnO are shown in Fig:(a–c). Bare ZnO and NiO particles are fine and quasi-spherical. The particles are revealed as relatively agglomerated, whereas the NiO/ZnO composite particles are shown in the dispersed mode. In binary oxide materials, particles appear to be bigger than in individuals. The NiO particles are decked on ZnO in ZnO/NiO. It is plausibly due to the Ni–O–Zn bonding character change. The dispersed surface structure has a higher surface area and positively influences the photocatalytic effectiveness of the material. Energy-dispersive X-ray spectroscopy was investigated to identify the elements present in the prepared materials. Figure 2. (d–f) shows the EDS elemental mappings corresponding to all NiO, ZnO, and NiO/ZnO samples. The presence of elements Ni and O in NiO, Zn, and O in ZnO; Ni, Zn, and O in NiO/ZnO are confirmed without any other impurity species.

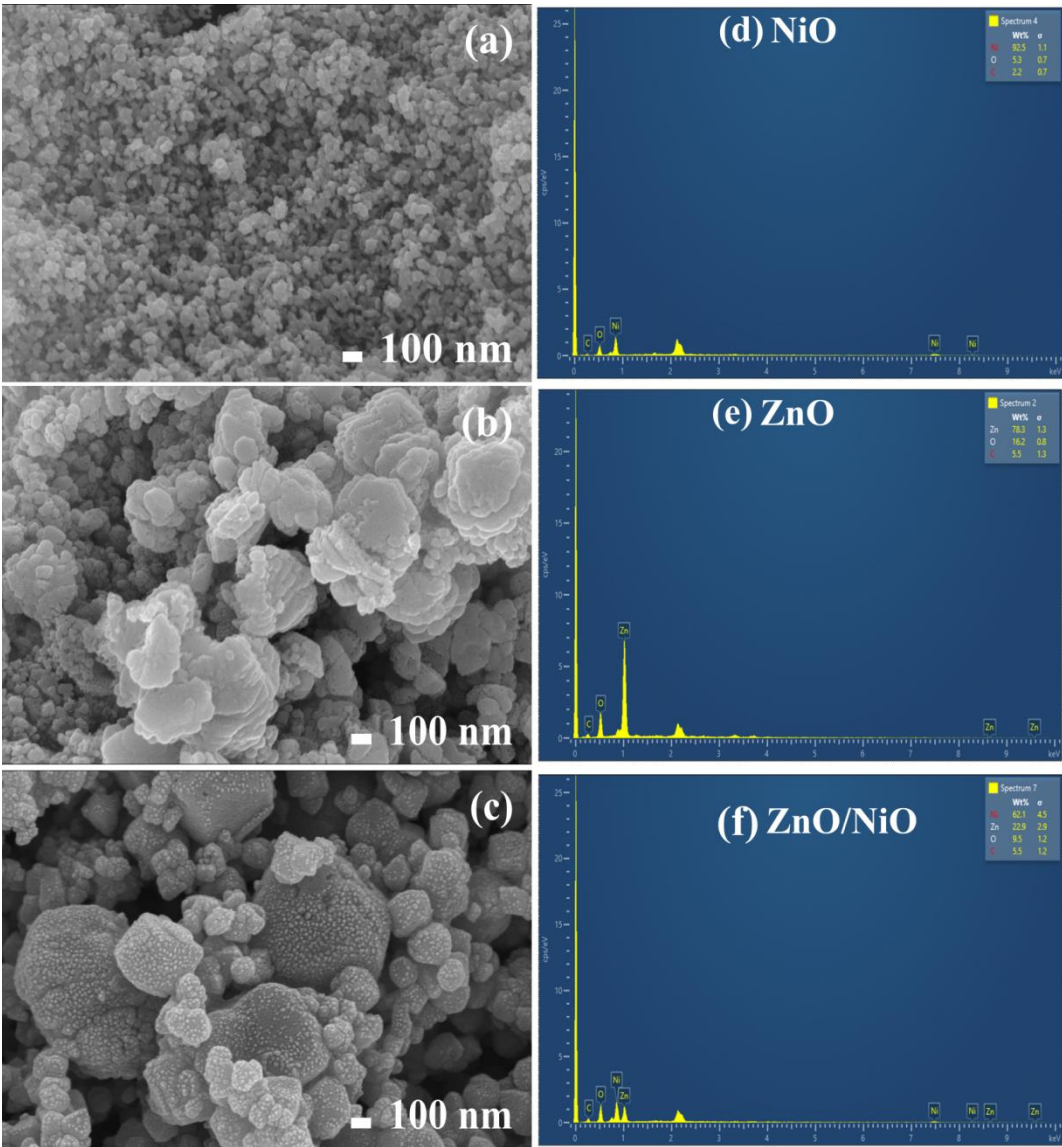


Fig.2. FESEM micrographs of (a) NiO, (b) ZnO, and (c) ZnO/NiO Nanoparticles and their EDS (d-f)

3.1.3 Optical Properties

The optical properties of NiO, ZnO, and ZnO/NiO materials were studied by UV-VIS absorption spectroscopy. The UV-visible absorption spectra of prepared samples NiO, ZnO, and ZnO/NiO are shown in Figure 3(a).

The UV-Vis absorbance of the ZnO/NiO composite obtained was higher than the NiO and ZnO nanoparticles, which implied that ZnO/NiO has relatively better light-harvesting efficiency. The result showed firm absorption peaks at 249, 243, and 236 nm

wavelengths for pure NiO, ZnO, and ZnO/NiO samples. The band gap energy of the prepared samples was evaluated using the Tauc plot and is presented in Figure 3(b). The energy band gaps of NiO, ZnO, and ZnO/NiO composites are 4.6, 5.1, and 5.2 eV, respectively.

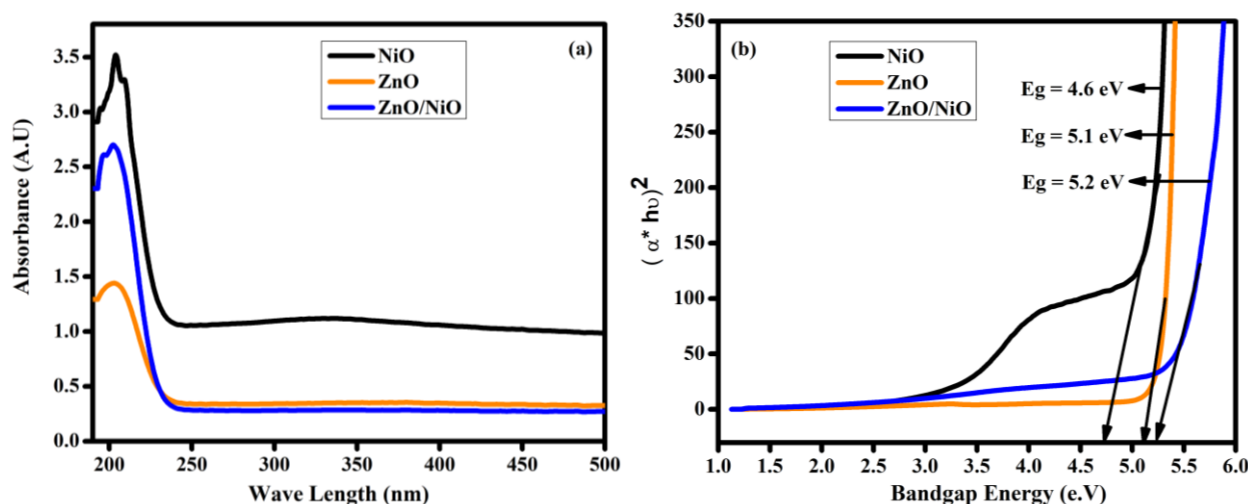


Fig.3. (a) UV- Visible spectra, (b) Tauc Plots of NiO, ZnO, and ZnO/NiO

3.1.4. Vibrational analysis

The Fourier Transform Infrared (FTIR) analysis defines the different functional groups in the prepared nanoparticles and nanocomposite. The obtained vibrational peaks are compared with the FTIR library, and functional groups such as carbonate, hydroxyl and metal oxide vibrational notes are found [13]. The FTIR spectrum of Nickel Oxide (NiO) exhibits characteristic peaks corresponding to the material's vibrational modes. Peak around $455\text{--}465\text{ cm}^{-1}$: This peak corresponds to the Ni-O stretching vibration. In the NiO crystal structure, the nickel and oxygen atoms are bonded, and this peak arises from the stretching of this Ni-O bond. Peak around $530\text{--}550\text{ cm}^{-1}$ is attributed to the Ni-O-Ni bending vibration. In the NiO lattice, the oxygen atoms are sandwiched between two nickel atoms, and the bending of this Ni-O-Ni arrangement gives rise to this peak. Peak around $725\text{--}735\text{ cm}^{-1}$ is associated with the Ni-O-Ni asymmetric stretching vibration. Similar to the previous peak, this mode involves stretching the Ni-O-Ni linkage but in an asymmetric manner. Peak around $840\text{--}860\text{ cm}^{-1}$ peak can be attributed to the Ni-O-Ni symmetric stretching vibration. In this case, the Ni-O-Ni linkage stretches symmetrically, leading to this higher frequency peak. Peak around $1400\text{--}1420\text{ cm}^{-1}$ is typically assigned to the presence of carbonate (CO_3^{2-}) species on the NiO surface. Carbonate can be introduced due to the adsorption of atmospheric CO_2 on the NiO surface [14-16].

It's important to note that the exact peak positions may vary slightly depending on factors such as the synthesis method, particle size, and experimental conditions. However, the general assignments mentioned above are widely accepted in the literature for the FTIR characterization of NiO [17-18]. The peak around $455\text{--}465\text{ cm}^{-1}$ corresponds to the Ni-O stretching vibration. The peak around $530\text{--}550\text{ cm}^{-1}$ is due to the Ni-O-Ni bending

vibration. The peak around $725\text{-}735\text{cm}^{-1}$ is assigned to the Ni-O-Ni asymmetric stretching vibration. The peak around $840\text{-}860\text{cm}^{-1}$ is associated with the Ni-O-Ni symmetric stretching vibration. The peak around $1400\text{-}1420\text{cm}^{-1}$ indicates the presence of carbonate species on the NiO surface.

FTIR spectra of Zinc Oxide (ZnO) typically exhibit distinct peaks that correspond to the characteristic vibrational modes of the material. Understanding these peaks provides valuable insights into the structure and properties of ZnO. The fundamental absorption peak around $400\text{-}500\text{cm}^{-1}$ corresponds to the fundamental lattice vibration mode of the ZnO crystal structure[19]. It arises from the stretching vibration of the Zn-O bond within the ZnO tetrahedra. The precise position of this peak is influenced by factors such as the crystallinity, defects, and doping of the ZnO material. The shoulder peak of ZnO could be observed in the range of $550\text{-}660\text{cm}^{-1}$ which might be due to the polycrystalline or nanostructure of ZnO and also attributed to the bending vibration of the Zn-O-Zn bond within the ZnO tetrahedral. The peaks around $1100\text{-}1200\text{cm}^{-1}$ correspond to the infrared-active optical phonon modes of the ZnO crystal structure[20]. They arise from the transverse optical (TO) and longitudinal optical (LO) phonon modes of the ZnO lattice. The position and splitting of these peaks can be influenced by factors such as doping, strain, and the presence of defects in the ZnO material. The presence of broad peaks in the range of $3300\text{-}3600\text{cm}^{-1}$ indicates the existence of hydroxyl groups on the surface of the ZnO material[21]. These OH groups can be adsorbed water molecules or surface hydroxyl groups formed during the synthesis or processing of the ZnO. The intensity and position of these peaks can provide information about the surface chemistry and the degree of hydroxylation of the ZnO[21-23]. The analysis of the FTIR spectra of ZnO, including the identification and interpretation of these characteristic peaks, is essential for understanding the material's structural, compositional, and surface properties[24,25]. This information is crucial for various ZnO applications, such as optoelectronics, sensors, catalysis, and energy storage devices.

In ZnO/NiO, the main peaks in the FTIR spectra of ZnO and NiO correspond to the fundamental lattice vibration mode, the bending vibration of the Zn-O-Ni, Zn-O-Zn bond and Ni-O-Ni, the infrared-active optical phonon modes, and the presence of hydroxyl groups on the surface of the material. Due to similar frequencies of Zn-O and Ni-O bond causes to overlapping in the composite. The position, intensity, and splitting of these peaks provide valuable insights into the structural, compositional, and surface characteristics of the ZnO/NiO sample.

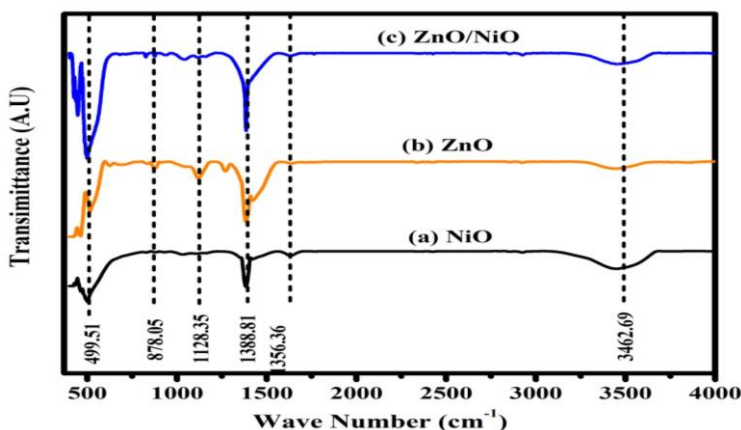


Fig.4. FTIR spectra of (a) NiO, (b) ZnO and (c) ZnO/NiO

4. Conclusions:

A summary of this study presents pure metal oxides (NiO and ZnO), and ZnO/NiO materials have been successfully prepared using the green method. The X-ray diffraction studies emphasized the development of cubic and hexagonal structures of ZnO/NiO composites. The metal oxides synthesized by the process described above possess high purity, as indicated by the XRD patterns. FESEM and EDS studied morphology and elemental investigations, respectively. The compositional analysis was studied using FTIR spectra. Band gap values confirming the obtained materials have a semiconductor band gap range.

Credit author statement

Akumarti Raju: Conceptualization, Methodology, Formal analysis, Investigation, Writing-original draft. Vangapandu Anusha: Data curation, Investigation. Budithi Ravi Kumar: Data curation, Investigation. Gattupalli Manikya Rao: Data curation, Formal analysis, Investigation.

Declaration of competing interest

The authors declare that they have no known competing financial interests or personal relationships that could have appeared to influence the work reported in this paper.

Data Availability Statement

The original contributions presented in the study are included in the article/Supplementary Material. Further inquiries can be directed to the corresponding author.

Acknowledgment

The authors acknowledge the Department of Physics, Andhra University, for providing the necessary facilities. The authors would like to express their sincere gratitude to Dr. Naresh Kumar. Rotte for his ongoing support through M/S. Regal Enterprises, Kamavarapukota-534449, Andhra Pradesh.

References

1. Advanced Sensor and Energy Materials ,Volume 2, Issue 3, September 2023, 100069 Preparations and applications of zinc oxide based photocatalytic materials panelYue Sun, Wei Zhang, Qun Li, Huijie Liu, Xiaolei Wang. <https://doi.org/10.1016/j.asems.2023.100069>.
2. Electrochimica Acta, Volume 502, 20 October 2024, 144860. Synthesis of NiO/ZnO/GO nanocomposites derived from Ni-Zn-H2BDC metal-organic framework for high performance supercapacitor electrodes. Fazeleh Mosaddegh, Hossein Esfandian, Mohammad Soleimani Lashkenari <https://doi.org/10.1016/j.electacta.2024.144860>.
3. Materials Science for Energy Technologies, Volume 8. Electrochemical applications of CdO-Co-ZnO nanocomposites, their synthesis and characterization reveal their multifunctional abilities.N. Rajkamal, K. Sambathkumar, K. Parasuraman, K. Bhuvaneswari, R. Uthrakumar, K. Kaviyarasu<https://doi.org/10.1016/j.mset.2024.07.002>
4. Materials Science and Engineering: B ,Volume 299, January 2024, 116935.A novel magnetic NiFe2O4-Ag-ZnO hybrid nanocomposite for the escalated photocatalytic dye degradation and antibacterial activitiesAmitender Singh, Fayu Wan, Kavita Yadav, Saarthak Kharbanda, Preeti Thakur, Atul Thakur . <https://doi.org/10.1016/j.mseb.2023.116935>.
5. Synthesis of nanocrystalline ZnO–NiO mixed metal oxide powder by homogeneous precipitation method November 2015, Ceramics International 42(3) Ravi Kant Sharma, Deepak Kumar, Ranjana Ghose. DOI:10.1016/j.ceramint.2015.11.081
6. Preparation and characterization of NiO, ZnO and NiO–ZnO composite nanofibers by electrospinning method October 2014 , Materials Chemistry and Physics 148(3):1029-1035.Petronela Pascariu Dorneanu, Anton Airinei, Niculae Olaru, Mihaela Homocianu.DOI:10.1016/j.matchemphys.2014.09.014.
7. Journal of Energy Storage, Volume 39, July 2021, 102591.Empowering smart grid: A comprehensive review of energy storage technology and application with renewable energy integration Kang Miao Tan, Thanikanti Sudhakar Babu, VignaK. Ramachandaramurthy, Padmanathan Kasinathan, Sunil G. Solanki, Shangari K. Raveendran <https://doi.org/10.1016/j.est.2021.102591>.
8. Chemosphere, Volume 264, Part 2, February 2021, 128580. A review on biosynthesis of metal nanoparticles and its environmental applications. Saravana, P.Senthil Kumar, S. Karishma, DaiVietN. Vo, S. Jeevanantham, P.R. Yaashikaa, Cynthia Susan George<https://doi.org/10.1016/j.chemosphere.2020.128580>.
9. X-Ray Powder Diffraction Scott T. Misture, in Encyclopedia of Materials: Technical Ceramics and Glasses, 2021.
10. International Journal of Management, Technology And Engineering, ISSN NO : 2249-7455. APPLICATION OF DEBYE-SCHERRER FORMULA IN THE DETERMINATION OF SILVER NANO PARTICLES SHAPE SWARNALATHA KURAPATI#1, PRATHIMA KUMARI SRIVASTAVA*2 CH. S. D. ST.
11. MIT Center for Materials Science and Engineering, Estimating Crystallite Size Using XRD, Scott A Speakman, Ph.D. 13-4009A speakman@mit.edu <http://prism.mit.edu/xray>.
12. XRD Crystallite (grain) Size Calculator (Scherrer Equation) – Insta NANO. <https://instanano.com/all/characterization/xrd/crystallite-size/> (accessed November 7th, 2024).
13. Fourier Transform Infrared Spectroscopy: Fundamentals and Application in Functional Groups and Nanomaterials Characterization, September 2018Shahid Ali Khan, Sher Bahadar Khan, Latif Ullah Khan, DOI:10.1007/978-3-319-92955-2_9
14. Applications of Fourier Transform-Infrared spectroscopy in microbial cell biology and environmental microbiology: advances, challenges, and future perspectives. Amin Kassem

- 1,✉, Lana Abbas 1, Oliver Coutinho 1, Somie Opara 1, Hawraa Najaf 1, Diana Kasperek 1, Keshav Pokhrel 2, Xiaohua Li 1, Sonia Tiquia-Arashiro 2023 Nov 21;14:1304081. doi: 10.3389/fmicb.2023.1304081.
15. Fourier transform infrared spectroscopy for molecular analysis of microbial cells Jesús J Ojeda 1, Maria Dittrich, PMID: 22639215, DOI: 10.1007/978-1-61779-827-6_8.
16. Morphological, chemical and structural characterisation of deciduous enamel: SEM, EDS, XRD, FTIR and XPS analysis. Eur J Paediatr Den 2014 Sep;15(3):275-80. C M Zamudio-Ortega 1, R Contreras-Bulnes 1, R J Scougall-Vilchis 1, R A Morales- Luckie 2 O F Olea-Mejía 2, L E Rodríguez-Vilchis, PMID: 25306144.
17. NiO Nanoparticles: Synthesis and Characterization , A. Rahdar* , a , M. Aliahmadb , Y. Azizi. JNS 5 (2015) 145- 151, Journal of NANOSTRUCTURES.
18. Results in Physics, Volume 6, 2016, Pages 1024-1030 Fabrication and characterization of semiconductor nickel oxide (NiO) nanoparticles manufactured using a facile thermal treatment, Manal Hashem, Elias Saion, Naif Mohammed Al-Hada, Halimah Mohamed Kamari, AbdulH. Shaari, Zainal Abidin Talib, Suriati B. Paiman, Mazliana A. Kamarudeen <https://doi.org/10.1016/j.rinp.2016.11.031>.
19. Nano-Structures & Nano-Objects, Volume 12, October 2017. Structural, optical and photocatalytic study of ZnO and ZnO–ZnS synthesized by chemical method. Gaurav Hitkari, Sandhya Singh, Gajanan Pandey. <https://doi.org/10.1016/j.nanoso.2017.08.007>.
20. International Journal of Science and Research (IJSR) ISSN (Online): 2319-7064 Index Copernicus Value (2013): 6.14. Vibrational Spectroscopy of ZnO-ZnS Nanoparticles. G. Janita Christobel.
21. Synthesis And Characterization Of Zinc Oxide Nanoparticles Using Green Synthesis Method. Archana A. Chaudhari , Umesh. J. Tupe , Arun V. Patil , Chandrakant. G. Dighavkar. International Journal Of Creative Research Thoughts (IJCRT) ISSN: 23202882.
22. Preparation and Characterization of Zinc Oxide Nanoparticles Using Leaf Extract of Sambucus ebulu. Sanaz Alamdari, Morteza SasaniGhamsari, Chan Lee, Wooje Han, Hyung-Ho Park, Majid Jafar Tafreshi, Hosein Afarideh and Mohammad Hosein Majies Ara Appl. Sci. 2020, 10(10), 3620; <https://doi.org/10.3390/app10103620>.
23. Synthesis, Characterization and Photocatalytic study of FeCr2O4@ZnO@MgO Core-Shell Nanoparticle. Ashok V. Borhade , Dipak R. Tope, Jyoti A. Agashe , Sachin S. Kushare. <https://doi.org/10.22090/jwent.2021.02.006>.
24. ZnO nanostructured materials and their potential applications: progress, challenges and perspectives. Sauvik Raha and Md. Ahmaruzzaman .DOI: 10.1039/D1NA00880C (Review Article) Nanoscale Adv., 2022, 4, 1868-1925.
25. Green synthesis of ZnO, CuO and NiO nanoparticles using Neem leaf extract and comparing their photocatalytic activity under solar irradiation. Lema Yadeta Gemachu, Asnake Lealem Birhanu, Article: 2293841. <https://doi.org/10.1080/17518253.2023.2293841>.